Catalysis Today 150 (2010) 196–206

Contents lists available at ScienceDirect

Catalysis Today

journal homepage: www.elsevier.com/locate/cattod

Bimetallic Co–Mo complexes: A starting material for high active hydrodesulfurization catalysts

Oleg V. Klimov *, Anastasiya V. Pashigreva, Galina A. Bukhtiyarova, Sergey V. Budukva, Martin A. Fedotov, Dmitri I. Kochubey, Yuri A. Chesalov, Vladimir I. Zaikovskii, Alexandr S. Noskov

Boreskov Institute of Catalysis SB RAS, pr. ak. Lavrentiev, 5, Novosibirsk 630090, Russia

ARTICLE INFO

Article history:
Available online 27 August 2009

Keywords:
Hydrotreatment catalyst preparation
Bimetallic Co–Mo complexes
Sulfide catalysis

ABSTRACT

The preparation of high active hydrodesulfurization catalysts is described. The procedure is based on the synthesis of labile bimetallic Co–Mo complexes in aqueous solution followed by the deposition on alumina surface at the conditions providing the structure of precursor remains unaltered after the drying. The prepared oxide surface compounds contain cobalt in the immediate vicinity of molybdenum that provides the selective formation of bimetallic sulfide compounds during the sulfidation. These compounds reveal the high activity in hydrotreatment of diesel fuels.

1. Introduction

The active component of supported hydrodesulfurization (HDS) catalyst consists of the surface bimetallic sulfide compound (usually denoted as CoMoS or NiMoS phase). Co (or its substitute Ni) atoms are chemically bonded to nanosize molybdenum sulfide particles of molybdenite structure. These particles have the shape of either the separate laminas or the multilayer stacks with Co atoms located at the edges and corners of the MoS_2 slabs [1]. Usually the modern high active commercial catalysts contain MoS_2 particles with the mean size of 28–58 Å [2], while for some model catalysts it was reported that the large fraction of surface MoS_2 forms the particle of less than 10 Å size [3]. Ideally, in the properly prepared catalyst cobalt should be incorporated totally into bimetallic sulfide compounds and the presence of the other substances (like Ni_3S_2, NiS, Co_9S_8, surface Mo and Co compounds with alumina) is to be minimized [1–3]. Several hypotheses concerning the actual localization of cobalt on MoS_2 particle were proposed [1–8], but many researchers have reported recently that in the activated catalysts the closest distance between Co and Mo atoms falls in the range of 2.75–2.85 Å [3–13]. This conclusion was based on the investigation of both the lab samples [3–6,11–13] and the commercial catalysts [7–10].

Thus, the commercially reasonable method of preparation of HDS catalyst should be capable to selectively synthesize the surface bimetallic sulfide compounds in the form of 20–60 Å long MoS_2 particles with the thickness of one or several layers. Co (or Ni) cations should be localized at the particle brims to achieve the spacing to the closest Mo atom of 2.75–2.85 Å.

The commercial HDS catalysts are prepared via the support impregnation by the aqueous solutions of Mo and Co substances of oxidic nature. The final structure of surface molybdenum disulfide is achieved at the last preparation stage, when the oxidic precursor is treated by various sulfur-containing agents. Then, both the size and morphology of the resulted MoS_2 particles are affected by the multitude of the factors, such as the chosen Mo compound, the influence of the chelate species, the structure and dispersion of oxide precursors, the nature of both the support itself and the support modifiers, the surface concentration of Mo species, the conditions of the sulfidation procedure. [8,13–15]. Nowadays the vast majority of the commercial HDS catalysts are based on alumina supports with the specific surface area of 200–300 m^2/g, and Mo loading is about 10–15% that roughly corresponds to 5–8 atoms per nm^2 [2]. Irrespective of the chosen sulfidation process, the most of MoS_2 particles in such catalysts are less than 60 Å long and have the average stacking number of 1–3 [2,13–16]. Thus, the preparation of surface Mo disulfide particles of the preferable size (20–60 Å) is well established process.

It is much more difficult to achieve the proper selective interaction between Co(Ni) and Mo in such a way as to promote their complete incorporation into the bimetallic sulfide compounds. Several processes could be employed for that: gas phase Co deposition over pre-synthesized MoS_2 particles [16], selective deposition of Co(Ni) onto surface Mo compounds from either aqueous or organic solutions [3] were reported for the lab prepared catalysts. Yet the mentioned procedures are rather complicated and could hardly be applied for the manufacturing of the commercial catalysts. In catalyst industry the desired dispersion and uniformity of the deposited components over the support

* Corresponding author. Tel.: +7 383 3333473; fax: +7 383 3308056.
E-mail addresses: klm@catalysis.ru (O.V. Klimov), pav@catalysis.ru (A.V. Pashigreva).

0920-5861/$ – see front matter © 2009 Elsevier B.V. All rights reserved.
doi:10.1016/j.cattod.2009.07.095

surface are attained by the calcination (i.e. high temperature annealing in air), but for HDS catalysts such treatment was reported to cause the formation of the large fraction of various Co(Ni) surface aluminates or molybdates that could not be converted to the desired Co(Ni)–Mo–S phase by the consequent sulfidation [4,8,17]. On the other hand, the sulfidation of not calcined catalysts containing the mixture of individual Co(Ni) and Mo substances yields the substantial amount of monometallic sulfides (MoS_2, Ni_3S_2, NiS and Co_9S_8), inactive in the hydrotreatment. Thus the proper catalyst design should provide the formation of the surface bimetallic compounds with the close spacing between Co(Ni) and Mo prior to the sulfidation step without calcination.

The most reasonable way to prepare such catalysts is the synthesis of bimetallic compounds containing Co(Ni) atoms in the vicinity of molybdenum in solution and the consequent deposition of these compounds to the support surface so that the structure of these complexes remains unaltered. As far as the best activity is demonstrated by the catalysts with Co(Ni)/Mo atomic ratio of 0.3–0.5, then complexes synthesized in solution should conform to this stoichiometry.

Recently several authors reported to use successfully bimetallic Co(Ni)–Mo compounds for the preparation of the supported HDS catalysts [11,17–27], but the characterization results proved that structure of bimetallic complexes remains unchanged after deposition stage are scarce presented in the literature [25–27].

Here we present the new HDS catalyst preparation method based on the application of the labile bimetallic Co–Mo aqueous complexes containing from two to three Mo atoms per one Co atom. The detailed deposition procedure was elaborated to provide the transfer of the bimetallic precursor from the solution to the alumina surface without its decomposition. The resulted catalysts were tested in ultra HDS of diesel.

2. Experimental

2.1. Synthesis of the bimetallic complexes in solution

The bimetallic complexes were synthesized from ammonia salts of the molybdenum-containing anions as follows: $[Mo_2O_4(C_2O_4)_2(H_2O)_2]^{2-}$ (obtained by the synthesis (as in [28]) of $(NH_4)_2[Mo_2O_4(OH)_4(H_2O)_2]$ and its following dilution in the equivalent amount of aqueous solution of oxalic acid); $[Mo_3O_4(C_2O_4)_3(H_2O)_3]^{2-}$ [29]; $[Mo_4O_{11}(C_6H_5O_7)_2]^{4-}$ [30] and $[H_2Mo_5P_2O_{23}]^{4-}$ [31]. Hereinafter the corresponding complexes are designated as Mo_2Ox, Mo_3Ox, Mo_4Citr and Mo_5P. For all the synthesis the solutions with same Mo concentration of [Mo] = 1.64 mol/dm^3 were used. Co was introduced by adding $Co(CH_3COO)_2\times4H_2O$ (for Mo_4Citr) and $Co(NO_3)_2\times6H_2O$ (for Mo_2Ox, Mo_3Ox and Mo_5P) to the aqueous solutions of Mo-containing components. The exact amounts of Co^{2+} were introduced to compensate the counter-charge of the corresponding anion. In the case of Mo_5P carbamide was added to the solution to achieve $Co^{2+}/(NH_2)_2CO$ ratio of 1.

Finally, bimetallic complexes were obtained with Co:Mo stoichiometry of 1:2 for Mo_2Ox and Mo_4Citr; 1:3 for Mo_3Ox and 2:5 for Mo_5P. These compounds are designated as $CoMo_2Ox$, $CoMo_3Ox$, $CoMo_4Citr$ and $CoMo_5P$. For the spectral studies the complexes were extracted from the solutions by the ethanol sedimentation.

2.2. Catalyst preparation

For the all samples the same alumina support was employed, i.e. the product of ZAO "Industrial catalysts", Ryazan, Russia. This support has specific surface area of 285 m^2/g, pore volume of 0.82 cm^3/g and average pore diameter of 115 Å. The support particles have the shape of trilobular bars with the circumscribed circle diameter of 1.5 mm and the length of 3–6 mm.

The catalysts were prepared with the special efforts to avoid the decomposition of precursor bimetallic complexes during its deposition over the support. The following procedure was employed: Schlenk flask with the weighed amount of the support was pumped out to 5 Torr, the pump was detached and the measured volume of bimetallic complex solution was introduced to exceed twice the water-absorbing capacity of the load. After 5 min the excess of solution was poured out and the catalyst was dried either in vacuum drying oven at room temperature ($CoMo_2Ox$, $CoMo_3Ox$), or in air at 110 °C ($CoMo_4Citr$ and $CoMo_5P$). The concentration of the solution was chosen to prepare the catalysts containing 11% Mo (as measured after their annealing at 550 °C). Note that the calcination was performed solely for the purpose of the precise evaluation of metals load and all other experiments were performed with not-calcined samples. The catalysts are mentioned below as $CoMo_2Ox/Al_2O_3$, $CoMo_3Ox/Al_2O_3$, $CoMo_4Citr/Al_2O_3$ and $CoMo_5P/Al_2O_3$.

The surface bimetallic compounds contain carboxylate ligands (bridging Co^{2+} and Mo-containing anions) as well as water ligands. The elimination of these ligands results in compacting of Co and Mo atoms and makes the catalyst samples more stable against electron beam used in HRTEM investigations. The removal of ligands was achieved by the extra drying of the catalysts in the flow of nitrogen at 400 °C for 2 h. These samples are designated by prefix N: $NCoMo_2Ox/Al_2O_3$, $NCoMo_3Ox/Al_2O_3$, $NCoMo_4Citr/Al_2O_3$ and $NCoMo_5P/Al_2O_3$.

The commercial alumina supported catalyst containing Mo 14.4%, Co 3.33% and B 0.45% with the same specific surface area as the catalysts prepared using bimetallic Co–Mo complexes was used to compare activity and stability with the synthesized catalysts for HDS of straight run gas oil (SRGO).

2.3. Sulfidation of the catalyst and its testing in HDS

The catalysts were crushed to a particle size of 0.25–0.5 mm, dried in nitrogen at 400 °C for 2 h and sulfided at 400 °C for 2 h at atmospheric pressure in H_2S at flow rate of 1000 ml/h. Sulfided catalysts are named with "S" prefix: $SCoMo_2Ox/Al_2O_3$ and so on.

After sulfidation the catalysts have been tested in HDS of SRGO (sulfur concentration—10500 wppm, density at 20 °C—0.855 g/ml and FBP—360 °C). The experiments were performed in the plug flow stainless steel reactor at 3.5 MPa, T = 320–375 °C, liquid hourly space velocity of 1.5–4.0 h^{-1} and H_2/feed volume ratio of 300–500. In such conditions the weight liquid product output was 94–96%, mainly due to the efficiency of the apparatus separator.

The sulfur content in the liquid products was measured by X-Ray Fluorescence Analyzer "LabX3500SL" "Oxford Instrument" and "Agilent 6890N" chromatograph equipped with an atomic-emission detector.

2.4. Complexes and catalyst characterization

2.4.1. NMR spectroscopy

NMR spectra at natural isotope abundance were recorded in AVANCE-400 Bruker spectrometer at the frequencies 26.06 (^{95}Mo), 100.4 (^{13}C), 161.98 (^{31}P) and 54.24 (^{17}O) MHz with accumulation rate of 45, 0.1, 0.1 and 45 Hz, respectively. The chemical shifts CS (in ppm) were referenced to the external standards of H_2O (^{17}O), tetramethylsilane (^{13}C), 85% H_3PO_4 (^{31}P) and 2 M solution of Na_2MoO_4 (^{95}Mo).

During the spectra acquisition the quality of the solutions (their color and transparency) remained unchanged. To study the interaction between Co and Mo-containing anions, Co nitrate or

acetate was dosed to the corresponding solution of Mo-containing substances so that Co:Mo ratio was ranged from 1:40 to 1:2.

2.4.2. FTIR spectroscopy

FTIR spectra of solid samples were recorded in transmission mode in KBr matrix with IR Fourier spectrometer Shimadzu FTIR 8300 with a resolution of 4 cm^{-1} (scans number was 50). Solid complex species (4 mg) and catalysts powder (40 mg) were mixed with 800 mg of KBr and pressed into wafers.

2.4.3. EXAFS spectroscopy

The EXAFS spectra of the Mo K-edge were obtained at the EXAFS Station of the Siberian Synchrotron Radiation Center (Novosibirsk) under the conventional transmission mode [32]. The storage ring VEPP-3 with the electron beam energy of 2 GeV and the average stored current of 100 mA was used as the source of radiation. The spectrometer has the Si (1 1 1) cut-off crystal-monochromator and two proportional ionization chambers as detectors. For each sample the oscillating portion of EXAFS spectra ($\chi(k)$) was treated in the form of $k^2\chi(k)$ at the wave number interval of 2.5–14.0 $Å^{-1}$. The EXAFS spectra simulations for retrieving of the structure data were performed by using the standard procedure by VIPER code [33]. The FEFF7 program was employed to fit the parameters of scattering [34].

2.4.4. HRTEM investigations

HRTEM images were obtained on a JEM-2010 electron microscope (JEOL, Japan) with a lattice-fringe resolution of 0.14 nm at an accelerating voltage of 200 kV. The high-resolution images of periodic structures were analyzed by the Fourier method. Local energy-dispersive X-ray analysis (EDX) was carried out on an EDAX spectrometer (EDAX Co.) fitted with an Si (Li) detector with a resolution of 130 eV. Samples to be examined by HRTEM were prepared on a perforated carbon film mounted on a copper grid. Particle size distribution was evaluated by means of iTEM 5.0 software.

3. Results and discussion

3.1. The synthesis of bimetallic complexes in solution and their structure

The synthesis of $CoMo_4Citr$ is described in [30,35] and its structure is depicted in Fig. 1. The core of the complex is tetranuclear $[Mo_4(C_6H_5O_7)_2O_{11}]^{4-}$ anion. The coordination of Co^{2+} cations was elucidated by NMR, FTIR and Raman spectroscopy. It was proved that two Co^{2+} cations were coordinated to the Mo-containing anion via the terminal oxygen atom, oxygen atom bonded with central atom of citric ligand and two carboxyl groups. In accordance with EXAFS data Co–Mo distance in the citrate complex is 3.41 Å.

It was shown in [25,26] that in the case of $CoMo_5P$ solution Co^{2+} cations are coordinated towards Mo-containing anion $[H_2Mo_5P_2O_{23}]^{4-}$ at Co–Mo distance of 3.65–3.66 Å, yet the details

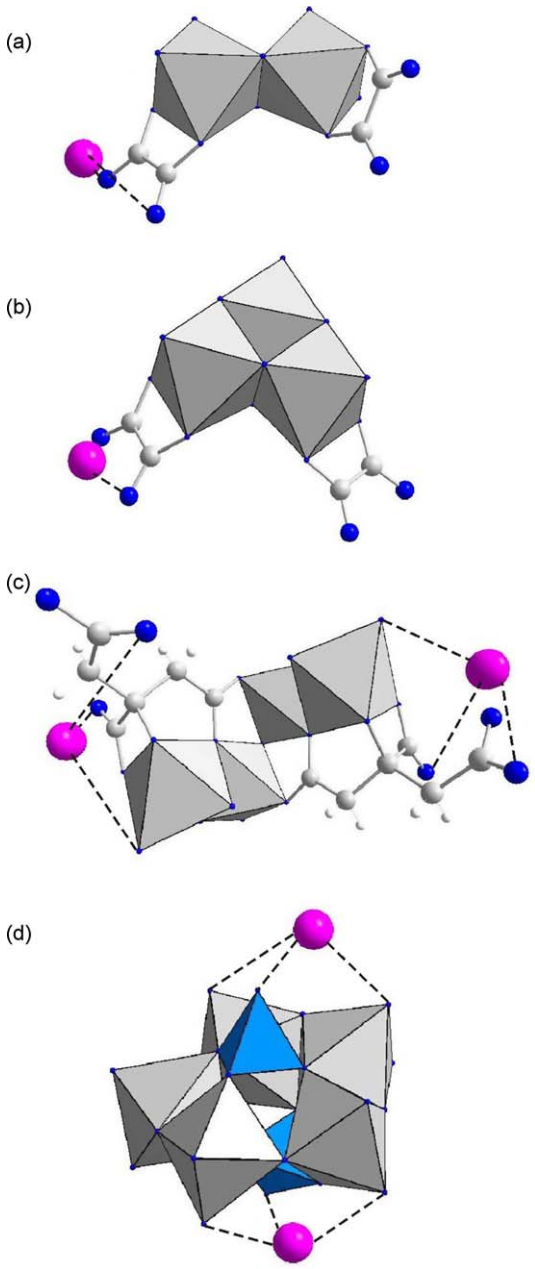

Fig. 1. Tentative structure of the bimetallic Co–Mo complexes: (a) $CoMo_2Ox$; (b) $CoMo_3Ox$; (c) $CoMo_4Citr$; (d) $CoMo_5P$, gray octahedra: MoO_6; blue tetrahedra: PO_4; pink ball Co atom; blue ball O atom; gray ball C atom. (For interpretation of the references to color in this figure legend, the reader is referred to the web version of the article).

of such coordination were not reported. We have studied the interaction of Co^{2+} and $[H_2Mo_5P_2O_{23}]^{4-}$ in solution earlier [36].

It was reported that the formation of heteropolyanion complexes with paramagnetic Co^{2+} cations leads to the shifting and broadening of NMR signals that depend on cobalt concentration in the solution [37]. In general, oxygen atoms coordinated to paramagnetic cations exhibit the more prominent changes in ^{17}O spectra. Indeed, for our samples all the spectra reveal some changes depending Co/Mo ratio in solution. ^{31}P and ^{95}Mo spectra demonstrate both the monotonic peaks broadening and the paramagnetic downfield shift (Table 1) similar to that ones reported in [26] while neither of the new peaks appears.

Since ^{17}O peaks from the different types of oxygen atoms are differently affected by the concentration of cobalt in the solution (see Fig. 2), the terminal oxygen atoms (Mo=O) and oxygen atoms

Table 1
^{95}Mo, ^{17}O and ^{31}P NMR data of the aqueous solutions of $CoMo_5P$.

Solution	^{95}Mo, δ (W)	^{31}P, δ (W)	^{17}O, δ (W)		
			O=Mo	Mo–**O**–Mo	^{17}O, P**O**$_4$
Without Co	12.6 ± 1 (260)	1.9 (90)	837 (160)	379 (320)	86 (490)
Co/Mo = 1/10	60 ± 2 (550)	13 (3700)	935 (1500)	380 (320)	97 (600)
Co/Mo = 1/5	180 ± 3 (830)	*	*	385 (380)	137 (870)
Co/Mo = 2/5	*	*	*	390 (540)	168 (1500)

δ—chemical shift, ppm; W—width of a line, hertz.
* —line is not visible because of broadening.

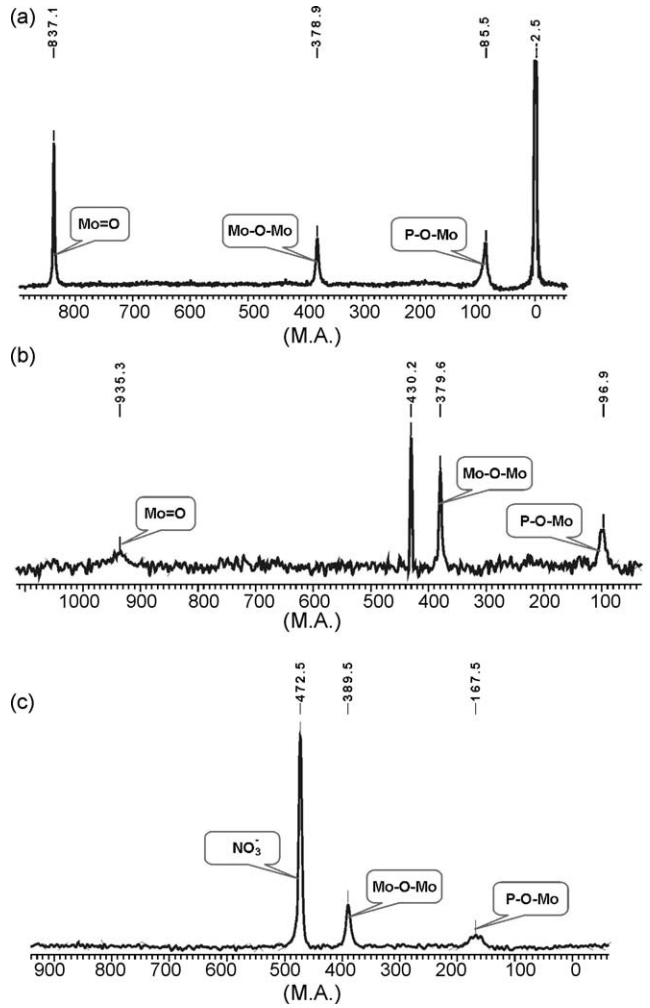

Fig. 2. ^{17}O NMR spectra of the solutions $CoMo_5P$ (a) and $CoMo_5P$ with different Co^{2+} addition: (b) Co/Mo = 1/10 and (c) Co/Mo = 2/5.

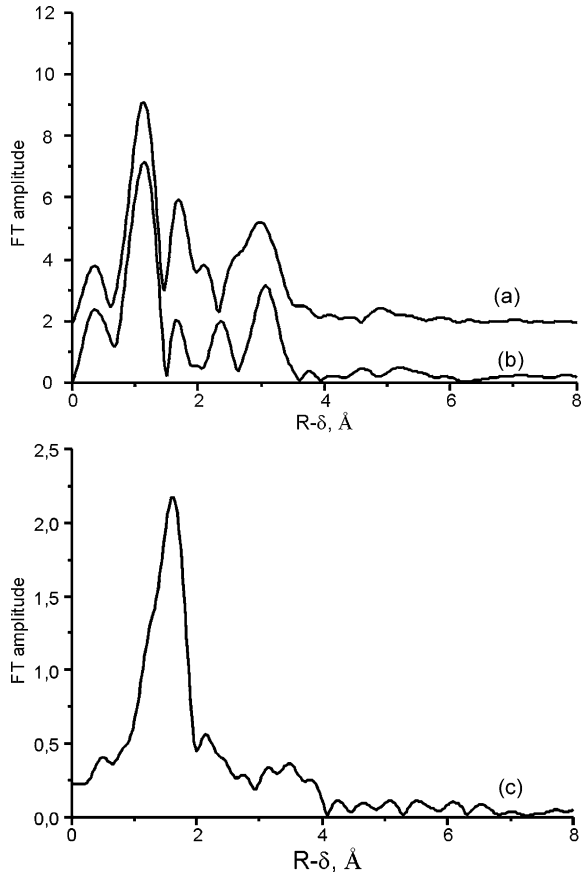

Fig. 3. Mo K-edge RDF curves for (a) $CoMo_5P$ solution; (b) $CoMo_5P/Al_2O_3$ and (c) (Co K-edge) $CoMo_5P$ solution.

of phosphate moieties are most sensitive, while the signal from bridged oxygen atoms (Mo–O–Mo) is changed slighter. ^{17}O spectra contain the narrow extra peak corresponding to oxygen in nitrate anion (introduced into the solution together with cobalt) with the peak position downshifted as compared with the diamagnetic salt solutions.

EXAFS data for $CoMo_5P$ solution are presented in Fig. 3. RDF curves around Mo K-edge are in the good agreement with that ones reported in [25] for $[H_2P_2Mo_5O_{23}]^{4-}$, but the distance between Mo and Co could hardly be evaluated. On the contrary, RDF curves for Co K-edge have the distinct maximum at 3.8 Å that could be attributed to Co–Mo spacing.

The combination of the changes in ^{95}Mo, ^{31}P and ^{17}O NMR spectra of $[H_2P_2Mo_5O_{23}]^{4-}$ solution caused by the addition of various amounts of Co^{2+} cations unambiguously indicates that the labile heteropolyanion–paramagnetic ion complexes are formed, in which the paramagnetic cations are coordinated to heteropolyanion via both the terminal Mo=O oxygen atoms and outer oxygen atoms of PO_4. In accordance with the structure of $[H_2P_2Mo_5O_{23}]^{4-}$ [38] the two most probable Co^{2+} atoms positions are above and below the plane of the molybdenum ring so that each Co ion is coordinated with one terminal oxygen from octahedral MoO_6 and with one outer oxygen atom from PO_4. The structure of $CoMo_5P$ is presented in Fig. 1 as well.

FTIR, EXAFS and NMR data obtained for Mo_2Ox solution agree exactly with the results of the previous investigations [28,39,40]. Upon the addition of various amounts of $Co(NO_3)_2 \times 6H_2O$ to Mo_2Ox solution NMR spectra reveal some changes induced by the effect of paramagnetic ligand (see Fig. 4 and Table 2). The peaks from terminal and bridged oxygen atoms have changed slightly whereas all the atoms of oxalate ligands demonstrate the strong broadening and paramagnetic shift. The only new peak appeared in NMR spectra is oxygen one from NO_3^- anion introduced into the solution together with cobalt. Neither the turbidity of the solution nor the sedimentation was noticed during the measurements. All peaks in Mo K-edge RDF curves below $R–\delta$ <4 Å are characteristic for the primary Mo_2Ox complex and remain unchanged after the addition of cobalt (Fig. 5).

The comparison of IR spectra (Table 3) for the Mo_2Ox and $CoMo_2Ox$ samples reveals the strong changes in the vibration modes of carboxyl groups due to the interaction of cobalt cations with oxalate ligands. The addition of cobalt nitrate to Mo_2Ox solution leads to the disappearing of the bands at 1709 and 910 cm^{-1} in the favor of the new band at 822 cm^{-1}. The modes corresponding to Mo–O vibrations remain unchanged. The most rational explanation of these spectral data is that oxalate ligands interact with Co^{2+} cations yet keeping their coordination towards Mo.

Thus it looks like the bimetallic complex formed in the solution containing cobalt cations coordinated towards $[Mo_2O_4(C_2O_4)_2(H_2O)_2]^{2-}$ via non-donor oxygen atoms of oxalate ligands. The supposed structure of $CoMo_2Ox$ is presented in Fig. 1. According to the structural data obtained for barium and potassium salts of the similar anion [41,42], the spacing between Co and Mo in $CoMo_2Ox$ should exceed 4 Å and the corresponding weak maximum in RDF curve should fall in the ($R–\delta$) range of 4.0–5.0 Å. Indeed, EXAFS

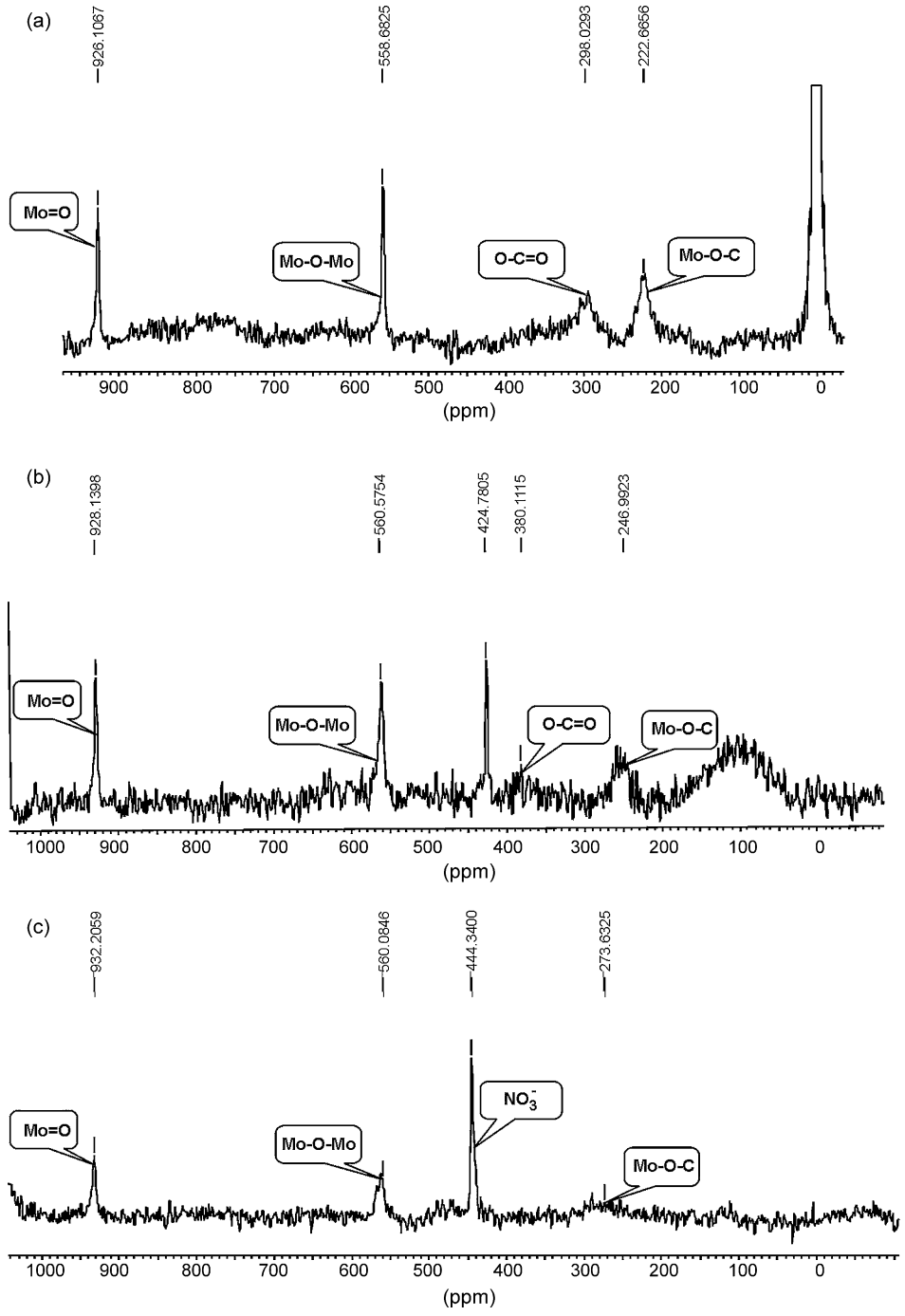

Fig. 4. ^{17}O NMR spectra of the Mo_2Ox solutions: (a) without Co; (b) Co/Mo = 1/10 and (c) Co/Mo = 1/2.

Table 2
^{95}Mo, ^{17}O and ^{13}C NMR data of the aqueous solutions of Mo_2Ox.

Solution	^{13}C, δ (W)	^{95}Mo, δ (W)	^{17}O, δ (W)			
			O=Mo	Mo–**O**–Mo	O–C=**O**	Mo–**O**–C
Without Co	166 (11)	531 (250)	926 (200)	559 (230)	298 (1800)	223 (800)
Co/Mo = 1/10	164.8 (430)	531 (330)	928 (230)	561 (500)	380 (4200)	247 (1300)
Co/Mo = 1/5	163.0 (920)	530	932 (270)	560 (680)	*	273 (2500)
Co/Mo = 1/2	161.3 (1560)	540	935 (280)	565 (700)	*	*

δ—chemical shift, ppm; W—width of a line, hertz.
* —line is not visible because of broadening.

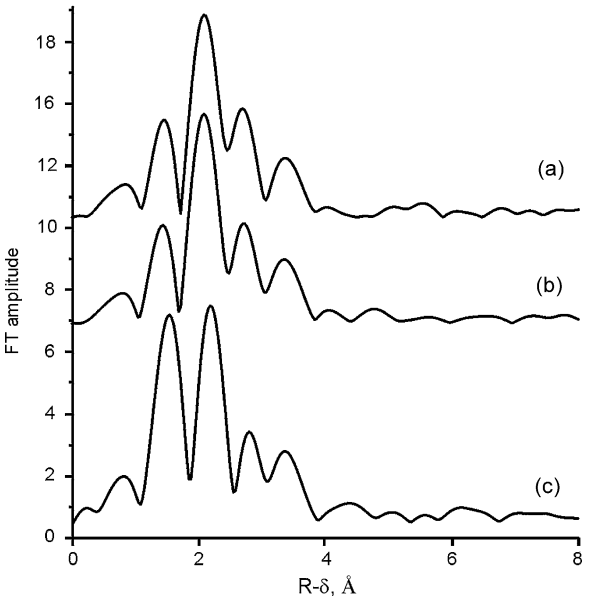

Fig. 5. Mo K-edge RDF curves for (a) Mo_2Ox solution; (b) $CoMo_2Ox$ solution and (c) $CoMo_2Ox/Al_2O_3$.

spectra contain several peaks in this region, but it is difficult to precisely attribute any of them to Co–Mo distance.

The spectral information gathered for Mo_3Ox sample is identical to that previously reported by us in [39,43,44]. The addition of cobalt nitrate to Mo_3Ox solution leads to the changes in NMR spectra similar to that ones observed in the case of Mo_2Ox (Table 4). The strongest broadening and paramagnetic shift was found for the atoms of oxalate ligands. The alteration of IR spectra for Mo_3Ox and $CoMo_3Ox$ resembles the changes noticed for the Mo_2Ox and $CoMo_2Ox$ samples (Table 5). Namely, the band at 1719 cm^{-1} had vanished and three bands at 1625, 1518 and 1444 cm^{-1} appeared instead. Mo–O vibration modes were not affected at all. Obviously, Co^{2+} cation is coordinated to $[Mo_3O_4(C_2O_4)_3(H_2O)_3]^{2-}$ anion via the oxalate ligand just in the same way as in $CoMo_2Ox$. Hypothetical structure of $CoMo_3Ox$ is depicted in Fig. 1. The structural data on cesium salt [45] show that the distance between Co and closest Mo atom should be larger than 4 Å. As far as Co/Mo molar ratio is 1/3 (i.e. coordination number ~0.33) the EXAFS signal is too weak to reliably determine Mo–Co distance.

3.2. Supported catalyst preparation

Generally the support particles used for the preparation of the commercial HDS catalysts have diameter of at least 1.5 mm. The impregnation of such industrial extrudates by Mo and Co solutions results in non-uniform depth distribution of supported metals due to the local pH variations and the interaction with the various hydroxyl moieties at alumina surface [24,46]. Besides that, the diverse surface Mo–Co compounds are formed inside the support pores. Extending the impregnation time favors to more homogeneous distribution of the components in the bulk of the granules but also causes the transfer of Al^{3+} cations to the solution. These ions react with Co and Mo compounds thus forming even more complex species at the surface of alumina. At the drying stage these species are partially decomposed [21–24] so that the surface composition of the synthesized catalysts becomes rather unpredictable.

The discussed problems could be avoided in some extent by using the fast vacuum impregnation procedure described above. This approach could be applied to the preparation of the large catalyst lots that was proven by the successful manufacturing of the commercial party of IC-GO-1 catalyst [47]. Besides the better uniformity, the vacuum impregnation prevents the crumbling of the support granules by the local pressure variations usually caused by capillary effect. The low-temperature drying of the catalysts also helps to keep the structure of primary bimetallic compounds unaltered after their deposition to the support thus providing the high uniformity of surface composition.

The residual solutions poured from the support after the impregnation of the precursor complexes are transparent and do not contain any sediments. NMR spectra of these solutions are

Table 3
IR spectra and frequencies assignment for Mo_2Ox, $CoMo_2Ox$ and $CoMo_2Ox/Al_2O_3$.

Assignment	Mo_2Ox	$CoMo_2Ox$	$CoMo_2Ox/Al_2O_3$
ν_{as}(C=O)	1709	–	1726
ν_{as}(COO) + δ(–NH)	1688–1632	1682–1637, 1617	1700–1620
ν_s(C–O) + ν(C–C)	1408	1405	1437, 1404
ν_s(C–O) + δ(O–C=O) + δ(–NH)	1282	1357, 1317, 1290	1359, 1316, 1307, 1283
ν(Mo=O)	1001, 963, 936	1002, 963, 936	1003, 980, 936
ν_s(C=O) + δ(O–C=O)	910	822	[a]
ν(Mo–O) + δ(O–C=O)	800, 739	799, 736	[a]
δ(OMoO)	613	614	[a]
ν(C–C)	534	–	[a]
δ(OMoO) + δ(O–C=O) + ring def.	485	487	[a]

[a] The range is overlapped with broad absorption band of alumina.

Table 4
^{95}Mo, ^{17}O and ^{13}C NMR data of the aqueous solutions of Mo_3Ox.

Solution	^{13}C, δ (W)	^{95}Mo, δ (W)	^{17}O, δ (W)			
			Mo–**O**–Mo	Mo–**O** < Mo_2	O–C=**O**	Mo–**O**–C
Without Co	168 (20)	1038 (320)	740 (240)	498 (250)	300 (1900)	241 (850)
Co/Mo = 1/10	165 (390)	1040 (400)	746 (280)	501 (400)	365 (3500)	258 (1200)
Co/Mo = 1/6	163 (820)	1045	750 (300)	506 (580)	370 (4000)	280 (2300)
Co/Mo = 1/3	160 (1400)	1040	755 (320)	510 (800)	*	*

δ—chemical shift, ppm; W—width of a line, hertz.
* —line is not visible because of broadening.

Table 5
IR spectra and frequencies assignment for Mo_3Ox, $CoMo_3Ox$ and $CoMo_3Ox/Al_2O_3$.

Assignment	Mo_3Ox	$CoMo_3Ox$	$CoMo_3Ox/Al_2O_3$
ν_{as}(C=O)	1719	–	1719
ν_{as}(COO) + δ(–NH)	1703, 1681	1705, 1683, 1625	1700, 1684, 1622
ν_s(C–O) + ν(C–C)	1394	1518, 1444, 1394	1526, 1457, 1410
ν_s (C–O) + δ(O–C=O) + δ(–NH)	1319, 1256	1312, 1277, 1047, 1014	1312, 1289, 1049, 1019
ν_s(C=O) + δ(O–C=O)	967, 904	967, 904	[a]
ν(Mo–O) + δ(O–C=O)	797, 752, 725	800, 753, 728	[a]
δ(OMoO)	680	680	[a]
ν(C–C)	537, 516	536, 517	[a]
δ(OMoO) + δ(O–C=O) + ring def.	480	480	[a]

[a] The range is overlapped with broad absorption band of alumina.

identical to the spectra of the primary solutions, so that neither of the new Mo compounds is formed during the impregnation.

Thus according to our EXAFS investigation the surface compounds of the catalysts dried at 110 °C or in vacuum conditions preserve the Co–Mo coordination typical for the precursor bimetallic complexes $CoMo_5P$, $CoMo_2Ox$ and $CoMo_3Ox$, correspondingly (see Figs. 3, 5 and 6). The interaction of $CoMo_4Citr$ with alumina was reported in details earlier and the total identity of $CoMo_4Citr$ structure in solution and at support surface had been proven [30,35]. As well, it was shown in [36] that $CoMo_5P$ keeps its structure upon the deposition to alumina. FTIR spectra of $CoMo_2Ox/Al_2O_3$ and $CoMo_3Ox/Al_2O_3$ indicate that the impregnation stage does not alter the coordination of cobalt towards Mo-containing anions via the oxalate ligands (Tables 3 and 5). Thus, the whole scope of the experimental results gives us the good evidence that all the primary bimetallic compounds could preserve its structure fairly unaltered after the properly performed deposition to alumina surface.

3.3. The study of the catalysts dried at 400 °C in nitrogen flow

Drying in nitrogen flow leads to the elimination of physically adsorbed and coordinated water and to the decomposition of the carboxylate ligands. Indeed, $NCoMo_4Citr/Al_2O_3$ probe contains 2.5% of carbonaceous residues whereas $NCoMo_2Ox/Al_2O_3$ and $NCoMo_3Ox/Al_2O_3$ samples have 0.55% and 0.59% of carbon, respectively. Note that it is quite possible that the most carbon fraction is bonded exclusively to the support rather than to molybdenum [48]. The RDF curves of Mo surrounding for the samples dried at 400 °C are presented in Fig. 7. Interatomic distances and coordination numbers are compiled in Tables 6 and 7. For all the catalysts RDF curves drastically differ as compared with low-temperature/vacuum dried samples, obviously due to the elimination of water and ligand molecules and consequently, the distortion of the structure of the surface compounds. However, all the curves exhibit the peak corresponding to the closest Mo–O distance of 1.70 ± 0.02 Å with coordination number of 2.1–2.5. RDF curves for $NCoMo_3Ox/Al_2O_3$ and $NCoMo_4Citr/Al_2O_3$ samples show the extra peak for Mo–O spacing of 1.96 ± 0.02 Å with coordination number about 5.

In R–δ range of 2.0–4.5 Å several peaks are observed that could be attributed to Mo–Al, Mo–Mo, Mo–Co pairs as well as to the distances between Mo and the oxygen atoms of the adjacent metal atoms. Since the coordination between cobalt cations and Mo-containing surface compounds is most important for us, the main efforts have been made to evaluate Mo–Co and Mo–Mo distances.

For all the samples Mo–Mo distances fall in the range of 2.56–2.90 Å and are very close to that ones determined for the primary bimetallic complexes in the solutions and for the supported

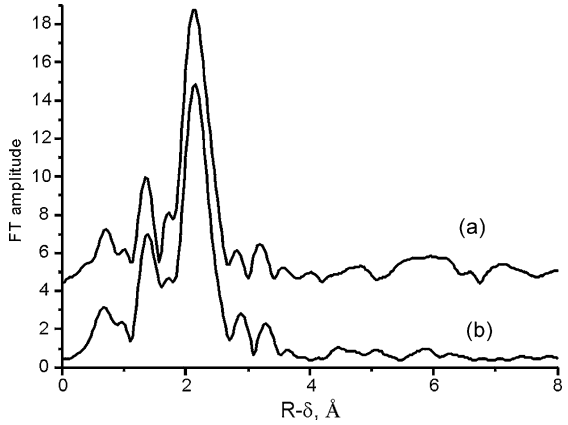

Fig. 6. Mo K-edge RDF curves for (a) $CoMo_3Ox$ and (b) $CoMo_3Ox/Al_2O_3$.

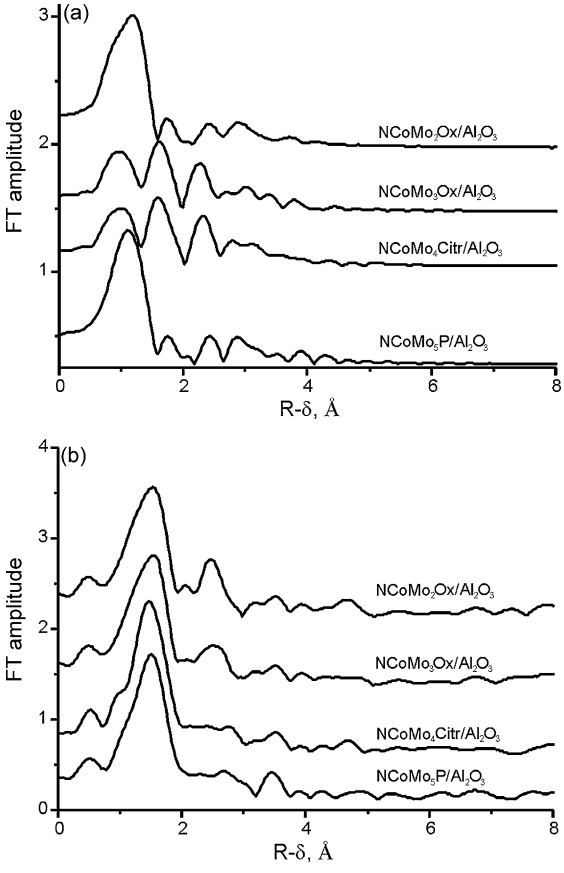

Fig. 7. RDF curves of catalysts after treatment in nitrogen at 400 °C. (a) Mo K-edge and (b) Co K-edge.

Table 6
Mo K-edge EXAFS parameters of catalysts after treatment in N_2, 400 °C.

Catalyst	Mo–O		Mo–O		Mo–Mo		Mo–Co	
	$R \pm 0.02$ (Å)	$N \pm 10\%$	$R \pm 0.02$ (Å)	$N \pm 10\%$	$R \pm 0.02$ (Å)	$N \pm 10\%$	$R \pm 0.02$ (Å)	$N \pm 10\%$
$NCoMo_2Ox/Al_2O_3$	1.68	2.2	–	–	2.90	0.5	4.05	0.4
$NCoMo_3Ox/Al_2O_3$	1.72	2.5	1.97	5.1	2.56	1.1	3.75	0.6
$NCoMo_4Citr/Al_2O_3$	1.72	2.1	1.96	5.2	2.60	1.3	3.82	0.7
$NCoMo_5P/Al_2O_3$	1.69	2.2	–	–	2.90	0.5	3.97	0.4

Table 7
Co K-edge EXAFS parameters of catalysts after treatment in N_2, 400 °C.

Catalyst	Co–O		Co–Mo	
	$R \pm 0.02$ (Å)	$N \pm 10\%$	$R \pm 0.02$ (Å)	$N \pm 10\%$
$NCoMo_2Ox/Al_2O_3$	2.00	2.9	3.83	1.0
$NCoMo_3Ox/Al_2O_3$	2.06	3.2	3.85	1.0
$NCoMo_4Citr/Al_2O_3$	2.01	3.3	3.85	1.5
$NCoMo_5P/Al_2O_3$	1.97	3.1	3.82	1.2

catalysts where molybdenum atoms are coordinated via the oxygen bridges (Table 5). Decrease of the coordination number values as compared with the initial complexes is caused by the disordering of Mo surrounding upon the elimination of ligands. Relatively slight difference of Mo–Mo distances before and after the heating probably indicates that heating does not affect the basic fragments of the primary complexes: Mo_2O_4, Mo_3O_4, Mo_4O_{11} and Mo_5O_{15} (for $NCoMo_2Ox/Al_2O_3$, $NCoMo_3Ox/Al_2O_3$, $NCoMo_4Citr/Al_2O_3$ and $NCoMo_5P/Al_2O_3$, respectively).

Since the Co/Mo molar ratio does not exceed 0.5 for all the samples, it is difficult to determine Mo–Co distance from EXAFS data for Mo K-edge. Our evaluations give the range of 3.75–4.05 Å for Mo–Co spacing with coordination numbers between 0.4 and 0.7. The estimation from Co K-edge spectra is more reliable (Fig. 7b and Table 7) and the same Co–Mo distance of 3.83 ± 0.02 Å was calculated for all the samples, whereas coordination numbers vary from 1.0 to 1.5. RDF curves for Co surrounding have intense peak attributed to Co–O spacing of about 2.0 Å—as well, for all the studied samples.

One should note that for $NCoMo_4Citr/Al_2O_3$ and $NCoMo_5P/Al_2O_3$ samples where the Co–Mo coordination was achieved by means of terminal oxygen atoms the distance between molybdenum and cobalt does not change significantly as compared to the primary bimetallic complexes. For $NCoMo_4Citr/Al_2O_3$ sample Co–Mo space is changed from 3.40 Å before drying to 3.83 Å for dried sample. For $CoMo_5P/Al_2O_3$ sample Co–Mo distance of 3.8 Å was not changed at all after the drying in the nitrogen flow.

On the contrary, $NCoMo_2Ox/Al_2O_3$ and $NCoMo_3Ox/Al_2O_3$ catalysts were prepared from the bimetallic complexes containing Co coordinated to Mo via oxalate ligands. For the fresh samples we have failed to measure Co–Mo distance from EXAFS data, yet after the drying the maximum appears in RDF curve that could be attributed to Co–Mo spacing of 3.83 ± 0.02 Å. We have mentioned above that for $CoMo_2Ox$ and $CoMo_3Ox$ complexes Co–Mo distance could be predicted from the structural information for alkaline metal salts [41,42,45] to exceed 4 Å. Then the observed lower value indicates obviously that decomposition of oxalate ligands leads to the compacting of Co and Mo in the surface compounds.

For all the studied catalysts the removal of both organic ligands and coordinated water provides the favorable conditions for the formation of the surface bimetallic clusters with the same metals stoichiometry as in the primary complexes. The size of such clusters should depend on the number of atoms in the primary bimetallic compounds. We cannot determine the precise positions of Co and Mo atoms at the support surface instrumentally but basing on our estimates of Mo–Mo and Co–Mo distances, the structural data reported in [38,41,42,45,49] and the values of ionic radii for Co^{2+}, Mo^{6+} and Mo^{4+} (1.64; 1.34 and 1.36 Å, respectively), we may conjecture to the dimensions of the supposed bimetallic clusters at alumina surface. Then the size of the smallest cluster consisting of one cobalt and two molybdenum atoms (i.e. $NCoMo_2Ox/Al_2O_3$ sample) should range from 4 Å (triangle layout) to 7 Å (in the case of linear atom arrangement). The size of largest clusters with Co_2Mo_4 and Co_2Mo_5 formulae ($NCoMo_4Citr/Al_2O_3$ and $NCoMo_5P/Al_2O_3$, respectively) should fall within 7–10 Å range.

The HRTEM image of $NCoMo_4Citr/Al_2O_3$ is presented in Fig. 8. Images for the rest samples are similar, so they are not presented in paper. The HRTEM pictures clearly demonstrate the bimetallic clusters as the high contrast spots evenly distributed over the smeared background of round-shaped alumina fragments. Despite the facts that microscope shows the bimetallic particles at different projections to the plane of the picture and the geometrical shape of the particle varies, the characteristic size of all the clusters falls within 4–10 Å interval. EDX data prove that the Co/Mo molar ratio in the clusters is the same as in the primary bimetallic complexes.

3.4. Sulfided catalysts

All the studied sulfided catalysts have S/Mo atomic ratio of 2.00 ± 0.05 thus proving their complete sulfidation.

HRTEM pictures of sulfided catalysts are presented in Fig. 9. All the catalysts demonstrate rather uniform distribution of Co, Mo and S over the alumina surface in accordance with EDX data. The presence of the particles of cobalt sulfides such as Co_9S_8 was not revealed in HRTEM images, analogically with described in [2]. The characteristics of the visible MoS_2 particles are presented in Table 8. For all the studied catalysts the particles of almost the same size of 35 Å and the average stacking number of 2.25 ± 0.15 were found. Such particle dimensions are typical for the effective HDS catalysts [2,13,15,16,50,51]. The number of MoS_2 layers in the slabs is slightly higher in our samples than in the catalysts described in the literature because of the gas phase sulfidation procedure we have

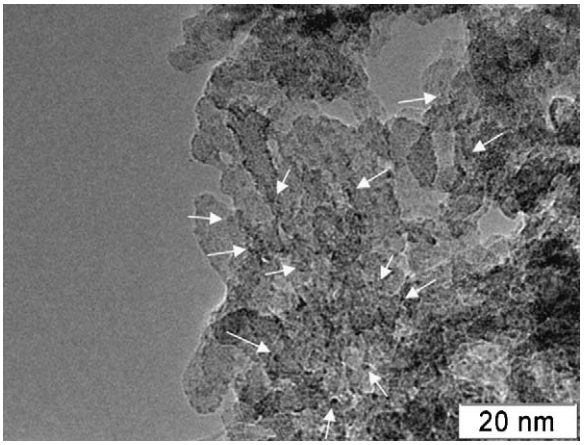

Fig. 8. HRTEM image of $NCoMo_4Citr/Al_2O_3$ catalyst after treatment in nitrogen at 400 °C. White arrows show the oxide CoMo clusters.

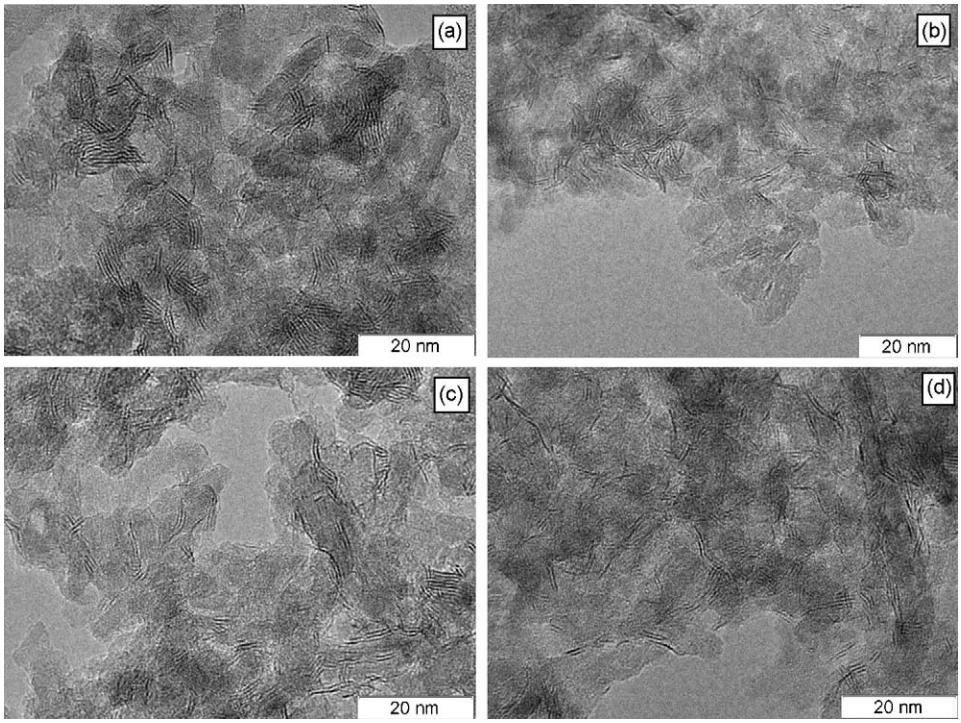

Fig. 9. HRTEM images of the catalysts after sulfidation: (a) $SCoMo_2Ox/Al_2O_3$; (b) $SCoMo_3Ox/Al_2O_3$; (c) $SCoMo_4Citr/Al_2O_3$ and (d) $SCoMo_5P/Al_2O_3$.

chosen. It is known that liquid phase sulfidation favors the formation of single-layer particles [2,50], but we took into account that the presence of multilayered particles enhance the HDS activity towards dibenzothiophene [15] or substituted dibenzothiophenes that appear to be the hardest transformable components in diesel fuels [52].

The radial distribution function curves of atoms around Mo and Co for the sulfided catalysts are presented in Fig. 10. All the investigated samples have two main peaks in the Mo K-edge RDF curves. The first one corresponds to the Mo–S distance of 2.40 ± 0.02 Å with the mean coordination number of 4.1. The second peak is attributed to Mo–Mo spacing of 3.16 ± 0.02 Å with coordination number of 2.55. Our estimations are in good agreement with the results reported in [3–13]. We did not tried to evaluate Mo–Co distance from Mo K-edge data since the coordination number is substantially lower than 1. Yet it is still possible to determine Co–Mo distance by means of Co K-edge spectral information. The two main maxima of Co K-edge RDF curves correspond to Co–S distance of 2.22 ± 0.02 Å (coordination number is 3.7–4.0) and to Co–Mo spacing of 2.78 ± 0.02 Å with coordination number between 0.8 and 1.0. Such distances and coordination numbers are typical for active sites of the hydrotreating catalysts, i.e. Co atoms located at the edge plane of MoS_2 particles [1–13]. The EXAFS Co K-edge data analysis did not reveal any distances that could be undoubtedly assigned to the oxygen containing compounds or cobalt sulfides CoS, CoS_2, Co_3S_4 and Co_9S_8, therefore it was concluded that all cobalt is included into sulfide bimetallic compounds.

Thus the obtained data of the element analysis, HRTEM, EDX and EXAFS for the sulfide catalysts allow to consider that morphology and the structure of surface bimetallic sulfide compounds are very similar in all the synthesized catalysts. The main component of all the prepared samples is fully sulfided Co–Mo compounds uniform distributed over alumina surface. All the cobalt atoms are located at the edge plane of MoS_2 particles with the average size of 35 Å and the average stacking number of 2.25 ± 0.15, the distance between Co and nearest Mo atom is 2.78 ± 0.02 Å. Such particle structure and dimensions are typical for the effective HDS catalysts and it is in good agreement with the properties of the hydrotreating catalysts active phase so-called CoMoS Phase Type II reported in the literature [1,2].

Table 8
MoS_2 morphology calculated from HRTEM micrographs.

Catalyst	Stacks number per 1000 nm^2	Average number of layers per stack	Average length (Å)
$SCoMo_2Ox/Al_2O_3$	68	2.35	30
$SCoMo_3Ox/Al_2O_3$	55	2.25	35
$SCoMo_4Citr/Al_2O_3$	52	1.95	40
$SCoMo_5P/Al_2O_3$	53	2.05	35

3.5. Catalytic properties

The catalytic testing results for our samples in HDS of SRGO are presented in Table 9. The particular interest was the comparison of catalytic properties of prepared samples with the well-known commercial hydroprocessing catalysts. The catalysts described in this paper were tested in the hydrotreatment of SRGO at liquid hour space velocity (LHSV) of 2.0 h^{-1}, H_2 pressure of 3.5 MPa and H_2/feed volume ratio of 300–500 nm^3/m^3. Such conditions are within the intervals of the flow rate (1.2–3.0 h^{-1}), pressure (3–4.5 MPa), temperature (340–380 °C) and H_2/feed volume ratio (250–500 nm^3/m^3) that are widely used for testing of the catalysts for deep HDS of SRGO both in the laboratory and in enlarged scale

Table 9
The results of SRGO hydrotreating activity of the studied catalysts.

Catalyst	Temperature for 50 ppm S fuel production (°C)	Temperature for 10 ppm S fuel production (°C)
$SCoMo_2Ox/Al_2O_3$	350	372
$SCoMo_3Ox/Al_2O_3$	353	370
$SCoMo_4Citr/Al_2O_3$	340	360
$SCoMo_5P/Al_2O_3$	355	375

3.5 MPa, liquid hourly space velocity of 2.0 h^{-1}, H_2/feed volume ratio of 300.

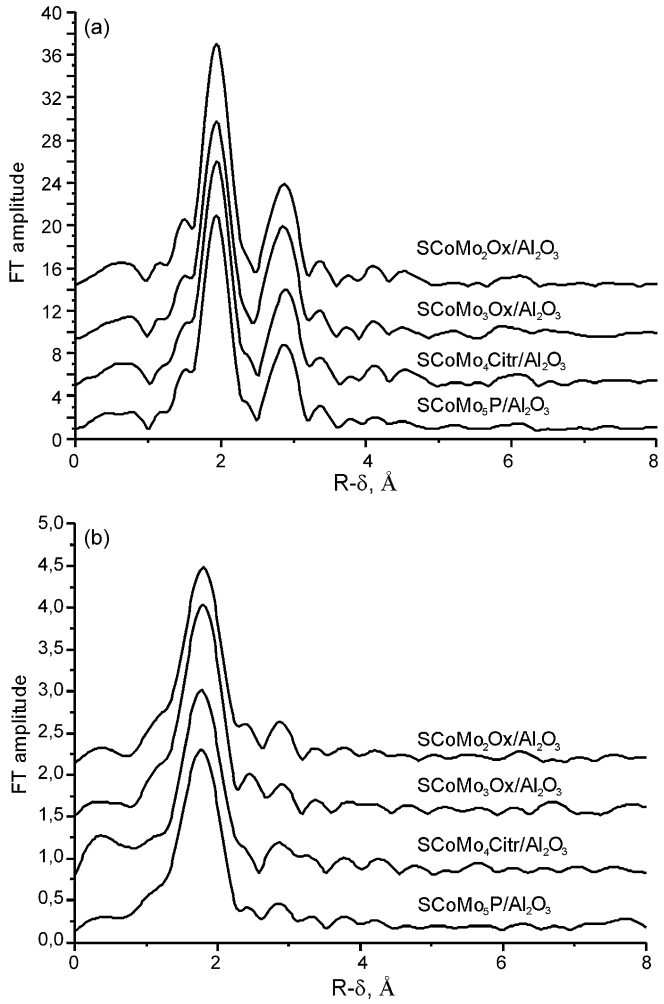

Fig. 10. RDF curves of catalysts after sulfidation: (a) Mo K-edge and (b) Co K-edge.

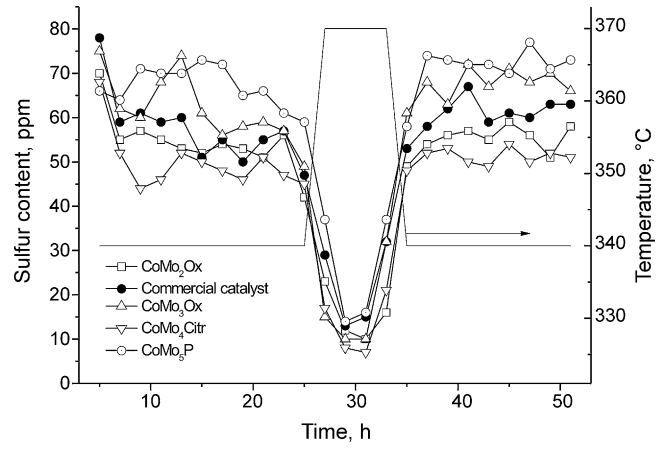

Fig. 11. The activity and stability of the catalysts prepared using bimetallic Co–Mo complexes in comparison with commercial catalyst in SRGO hydrotreatment.

[2,50,52–60]. The diesel fuels with residual sulfur content from 10 to 100 ppm are normally obtained in the presence of the commercial catalysts used in industry (KF-757 Stars, TK-554, TK-574, TK-576 BRIM, C-606A, 424 T @ and 448 T @) at the above specified conditions. For the commercial Russian catalysts used in oil-refining plants (RC-231, RC-242, NCYU-232, NCYU-500, GCD-205 and GCD-300) the residual sulfur content is much higher and lies in the range of 100–500 ppm [56–60]. The activity tests of the synthesized catalysts in HDS of SRGO showed that any of our catalysts is capable to yield the diesel with residual sulfur content of 10–80 ppm under comparable conditions. Thus, it was concluded that the activity of our catalysts is competitive with the activity of the well-known commercial catalysts for ultra-low sulfur diesel and significantly higher than that of the common brands of Russian catalysts.

To study the stability of the catalysts prepared using bimetallic Co–Mo complexes, they were tested in a special program [36], and one of the wildly used commercial catalysts successfully operated at Russian oil-refining plants was used as comparison sample. The samples were run 24 h at 340 °C, 8 h at 370 °C and at last again 24 h at 340 °C. The obtained test results are shown in Fig. 11.The temperature and the duration of the second stage were chosen to simulate the industrial conditions favorable for the formation of the carbonaceous deposits that cause the catalyst deactivation [61,62]. Our exploration revealed that the residual sulfur content on the final testing stage is just 3–5 ppm higher than at the beginning at 340 °C. Thus, our catalysts are not inferior in resistance to the decontamination to the one of the highly active hydrotreating commercial catalysts.

4. Conclusion

The synthesis of labile bimetallic Co–Mo complexes in the aqueous solution is presented. The bimetallic compounds with Co/Mo atomic ratio between 1:3 and 1:2 (i.e. the same stoichiometry as in the best reported HDS catalysts) were synthesized by coordination of Co^{2+} cations towards Mo-containing anions as follows: $[Mo_2O_4(C_2O_4)_2(H_2O)_2]^{2-}$, $[Mo_3O_4(C_2O_4)_3(H_2O)_3]^{2-}$, $[Mo_4O_{11}(C_6H_5O_7)_2]^{4-}$ and $[H_2Mo_5P_2O_{23}]^{4-}$.

Depending on the chosen anion, one of two basic types of cobalt coordination takes place:

1. In the case of $[Mo_4O_{11}(C_6H_5O_7)_2]^{4-}$ and $[P_2Mo_5O_{23}]^{6-}$ cobalt cations are coordinated to Mo-containing anions via terminal oxygen atoms and carboxyl (or phosphate) group;
2. In the case of $[Mo_2O_4(C_2O_4)_2(H_2O)_2]^{2-}$ and $[Mo_3O_4(C_2O_4)_3(H_2O)_3]^2$ cobalt cations are coordinated to Mo-containing anions via non-donor oxygen atoms of oxalate ligands.

The combination of the fast impregnation of vacuumized alumina extrudates and the low-temperature (<110 °C) drying allows to avoid the decomposition of bimetallic compounds upon the deposition to the support.

All the catalysts dried in the flow of nitrogen at 400 °C contain the nanosize (<10 Å) bimetallic clusters with rather short Co–Mo spacing of 3.8 Å.

The sulfidation of the synthesized supported catalysts yields the bimetallic sulfide particles with the average size of 30–40 Å and the mean stacking number of 1.95–2.35 evenly dispersed over the alumina surface. All the sulfided catalysts exhibit the same Co–Mo structure with Co–Mo spacing of 2.78 ± 0.02 Å and the coordination number of 0.8–1.0. The surface composition of the obtained samples is typical for the modern highly active hydrotreating catalysts, containing CoMoS Phase Type II as an active phase.

The catalysts demonstrate the high activity in HDS of SRGO. Any of our catalysts is capable to yield the diesel with less than 50 and 10 ppm. The studied catalysts are competitive with the activity and stability of the best commercial catalysts for ultra-low sulfur diesel production.

Thus the preparation procedure was elaborated for the synthesis of high active HDS catalysts, which can be used in the development of new industrial hydrotreating catalysts.

References

[1] H. Topsoe, B.S. Clausen, F.E. Massoth, in: J.R. Anderson, M. Boudart (Eds.), Hydrotreating Catalysis—Science, Technology, vol. 11, Springer-Verlag, New York/Berlin, 1996.
[2] S. Eijsbouts, L.C.A. Van den Oetelaar, R.R. Van Ruijenbroek, J. Catal. 229 (2005) 352.
[3] A.N. Startsev, Sulfide Hydrotreating Catalysts: Synthesis, Structure, Properties, Academic Publishing House "GEO", Novosibirsk, 2007, 206 pp..
[4] J.V. Lauritsen, J. Kibsgaard, G.H. Olesen, P.G. Moses, B. Hinnemann, S. Helveg, J.K. Norskov, B.S. Clausen, H. Topsoe, E. Laegsgaard, F. Besenbacher, J. Catal. 249 (2007) 220.
[5] A.N. Startsev, J. Mol. Catal. A: Chem. 152 (2000) 1.
[6] S.P.A. Louwers, R. Prins, J. Catal. 133 (1992) 94.
[7] B.R.G. Leliveld, J.A.J. van Dillen, J.W. Geus, D.C. Koningsberger, M. de Boer, J. Phys. Chem. B 101 (1997) 11160.
[8] S. Eijsbouts, Appl. Catal. A: Gen. 158 (1997) 53.
[9] J.T. Miller, C.L. Marshall, A.J. Kropf, J. Catal. 202 (2001) 89.
[10] J.T. Miller, W.J. Reagan, J.A. Kaduk, C.L. Marshall, A.J. Kropf, J. Catal. 193 (2000) 123.
[11] I. Pettiti, I.L. Botto, C.I. Cabello, S. Colonna, M. Faticanti, G. Minelli, P. Porta, H.J. Thomas, Appl. Catal. A: Gen. 220 (2001) 113.
[12] S.M.A.M. Bouwens, J.A.R. van Veen, D.C. Koningsberger, V.H.J. de Beer, R. Prins, J. Phys. Chem. 95 (1991) 123.
[13] A.I. Dugulan, E.J.M. Hensen, J.A.R. van Veen, Catal. Today 130 (2008) 126.
[14] E. Payen, R. Hubaut, S. Kasztelan, O. Poulet, J. Grimblot, J. Catal. 147 (1994) 123.
[15] E.J.M. Hensen, P.J. Kooyman, Y. van der Meer, A.M. van der Kraan, V.H.J. de Beer, J.A.R. van Veen, R.A. van Santen, J. Catal. 199 (2001) 224.
[16] T. Usman, T. Yamamoto, Y. Kubota, Okamoto, Appl. Catal. A: Gen. 328 (2007) 219.
[17] P. Blanchard, C. Lamonier, A. Griboval, E. Payen, Appl. Catal. A: Gen. 332 (2007) 33.
[18] C.I. Cabello, F.M. Cabrerizo, A. Alvarez, H.J. Thomas, J. Mol. Catal. A: Chem. 186 (2002) 89.
[19] C.I. Cabello, I.L. Botto, H.J. Thomas, Appl. Catal. A: Gen. 197 (2000) 79.
[20] N.N. Tomina, P.A. Nikulshin, A.A. Pimerzin, Kinet. Catal. 49 (2008) 653.
[21] C. Lamonier, C. Martin, J. Mazurelle, V. Harle, D. Guillaume, E. Payen, Appl. Catal. B: Environ. 70 (2007) 548.
[22] J. Mazurelle, C. Lamonier, C. Lancelot, E. Payen, C. Pichon, D. Guillaume, Catal. Today 130 (2008) 41.
[23] C. Martin, C. Lamonier, M. Fournier, O. Mentre, V. Harle, D. Guillaume, E. Payen, Chem. Mater. 17 (2005) 4438.
[24] J.A. Bergwerff, T. Visser, B.M. Weckhuysen, Catal. Today 130 (2008) 117.
[25] D. Nicosia, R. Prins, J. Catal. 229 (2005) 424.
[26] D. Nicosia, R. Prins, J. Catal. 234 (2005) 414.
[27] A. Griboval, P. Blanchard, E. Payen, M. Fournier, J.L. Dubois, Catal. Today 45 (1998) 277.
[28] A.N. Startsev, O.V. Klimov, S.A. Shkuropat, M.A. Fedotov, S.P. Degtyarev, D.I. Kochubey, Polyhedron 13 (1994) 505.
[29] W. Wardlaw, W.H. Parker, J. Chem. Soc. 127 (1925) 1311.
[30] O.V. Klimov, A.V. Pashigreva, D.I. Kochubei, G.A. Bukhtiyarova, A.S. Noskov, Doklady Phys. Chem. 424 (2009) 35.
[31] L. Pettersson, I. Andersson, L.-O. Ohman, Inorg. Chem. 25 (1986) 4726.
[32] D.I. Kochubey, EXAFS-Spectroscopy of the Catalysts, Science, Novosibirsk, 1992, p. 144.
[33] K.V. Klementev, J. Phys. D: Appl. Phys. 34 (2001) 209.
[34] J.J. Rehr, A.L. Ankudinov, Radiat. Phys. Chem. 70 (2004) 453.
[35] A.V. Pashigreva, Co-Mo hydrodesulfurization catalysts prepared via bimetallic complexes synthesis, PhD Thesis, Boreskov Institute of Catalysis SB RAS, Novosibirsk, 2009.
[36] M.A. Fedotov, O.V. Klimov, V.V. Kriventsov, E.A. Paukshtis, A.A. Budneva, A.V. Kalinkin, E.G. Kodenev, D.G. Aksenov, G.V. Echevsky, G.A. Bukhtiyarova, Proc. 8th EUROPACAT, Turku, Finland, 2007, pp. 9–21.
[37] A.K. Cheetham, N.J. Clayden, C.M. Dobson, R.J.B. Jakeman, J. Chem. Soc., Chem. Commun. (1986) 195.
[38] B. Hedman, Acta Chem. Scand. 27 (1973) 3335.
[39] O.V. Klimov, M.A. Fedotov, A.N. Startsev, J. Catal. 139 (1993) 142.
[40] A.N. Startsev, O.V. Klimov, S.A. Shkuropat, P.E. Kolosov, V.K. Fedorov, S.P. Degtyarev, D.I. Kochubei, React. Kinet. Catal. Lett. 41 (1990) 339.
[41] B. Kamenar, B. Kaitner, N. Strukan, Croatica Chem. Acta 64 (1991) 329.
[42] N. Strukan, M. Cindric, B. Kamenar, Acta Crystallogr. C 56 (2000) 639.
[43] O.V. Klimov, E.A. Krivoshchekova, A.N. Startsev, React. Kinet. Catal. Lett. 42 (1990) 95.
[44] O.V. Klimov, M.A. Fedotov, D.I. Kochubei, S.P. Degtyarev, A.V. Kalinkin, A.N. Startsev, Kinet. Catal. 36 (1995) 297.
[45] E. Benory, A. Bino, D. Gibson, F.A. Cotton, Z. Dori, Inorg. Chim. Acta 99 (1985) 137.
[46] J.A. Bergwerff, T. Visser, B.R.G. Leliveld, B.D. Rossenaar, K.P. de Jong, B.M. Weckhuysen, J. Am. Chem. Soc. 126 (2004) 14548.
[47] O.V. Klimov, A.V. Pashigreva, G.A. Bukhtiyarova, V.N. Kashkin, A.S. Noskov, G.M. Shragina, V.A. Sysoev, S.A. Sergienko, V.T. Liventsev, Ya.M. Polunkin, Proc. 8th Russian Oil, Gas and Energy International Forum, 8–10 April 2008, RESTEC, St. Petersburg, (2008), p. 274.
[48] A.V. Pashigreva, G.A. Bukhtiyarova, Yu.A. Chesalov, G.S. Litvak, O.V. Klimov, A.S. Noskov, Catal.Today (2009), doi:10.1016/j.cattod.2009.07.096.
[49] N.W. Alcock, M. Dudek, R. Grybos, E. Hodorowicz, A. Kanas, A. Samotus, J. Chem. Soc., Dalton Trans. (1990) 707.
[50] N. Frizi, P. Blanchard, E. Payen, P. Baranek, C. Lancelot, M. Rebeilleau, C. Dupuy, J.P. Dath, Catal. Today 130 (2008) 32.
[51] B. Guichard, M. Roy-Auberger, E. Devers, C. Legens, P. Raybaud, Catal. Today 130 (2008) 97.
[52] T. Fujikawa, H. Kimura, K. Kiriyama, K. Hagiwara, Catal. Today 111 (2006) 188.
[53] H. Topsoe, B. Hinnemann, J.K. Norskov, J.V. Lauritsen, F. Besenbacher, P.L. Hansen, G. Hytoft, R.G. Egeberg, K.G. Knudsen, Catal. Today 107–108 (2005) 12.
[54] K.G. Knudsen, B.H. Cooper, H. Topsoe, Appl. Catal. A: Gen. 189 (1999) 205.
[55] EPA-Diesel RIA, Regulatory Impact Analysis: Heavy-Duty Engine and Vehicle Standards and Highway Diesel Fuel Sulfur Control Requirements, United States Environmental Protection Agency, Air and Radiation, EPA420-R-00-026, December 2000.
[56] V.G. Rassadin, O.V. Durov, G.G. Vasil'ev, N.G. Gavrilov, O.Yu. Shlygin, N.M. Likhterova, Chem. Technol. Fuels Oils 43 (2007) 1.
[57] G.G. Vasil'ev, O.V. Durov, V.G. Rassadin, N.G. Gavrilov, O.Yu. Shlygin, N.M. Likhterova, Chem. Technol. Fuels Oils 43 (2007) 12.
[58] V.K. Smirnov, K.N. Irisova, E.L. Talisman, A.V. Efremov, M.I. Basyrov, O.V. Trofimov, Neftepererab. Neftekhim. 6 (2007) 13.
[59] O.V. Levin, A.G. Oltyrev, A.B. Golubev, V.A. Vyazkov, V.N. Seleznev, V.V. Samsonov, A.A. Lamberov, Catal. Ind. 1 (2004) 25.
[60] O.V. Klimov, A.V. Pashigreva, G.A. Bukhtiyarova, V.N. Kashkin, A.S. Noskov, Ya.M. Polunkin, Catal. Ind. 1 (2008) 6 (special issue).
[61] E. Furimsky, F.E. Massoth, Catal. Today 52 (1999) 381.
[62] M. Marafi, A. Stanislaus, Appl. Catal. A: Gen. 159 (1997) 259.